Adatom-step interactions: Atomistic simulations and elastic models

L. E. Shilkrot and D. J. Srolovitz
Department of Materials Science and Engineering, University of Michigan, Ann Arbor, Michigan 48109-2136
(Received 6 June 1996)

We derive an analytical expression for the interaction energy between an adatom and a step within the framework of linear elasticity. There are two unknowns in this theory: the strength of the elastic fields associated with the adatoms and the strength of the fields associated with the steps. In order to determine these parameters independently, we perform a series of atomistic simulations of a square lattice of Ni adatoms and a regular array of steps on the nominal (001) Ni surface using embedded-atom method potentials. The results are shown to yield good agreement with elastic theory. Fitting these simulations to the theory allows us to determine the adatom and step strengths. These results are then used to predict the step-adatom interaction energy. Atomistic simulations of a surface with a periodic array of steps interacting with an adatom are performed and compared with the predictions of the elastic theory with no adjustable parameters. A comparison of simulation and theory shows that the step-adatom interactions are dominated by dipole-dipole interactions, but that higher-order terms can also be significant. However, the absolute magnitude of the step-adatom interaction energy show significant errors. We believe that these errors are associated with the neglect of anisotropic effects in the elastic analysis used to extract that adatom dipole strength. [S0163-1829(97)05607-5]

I. INTRODUCTION

Interactions between adsorbed atoms as well as interactions with other types of defects on metallic surfaces have been widely studied[1] because of the importance of this problem for the understanding of epitaxial crystal growth and surface morphology evolution processes.[2] Recently developed microscopy techniques have made it possible to make direct observations of interacting adatoms and surface steps.[3] However, despite this prolonged interest, the fundamental nature of these interactions is still not fully understood. In the present paper, we examine the long-range interactions between adatoms and between adatoms and steps on a surface using both atomistic computer simulation and elastic theory. Such a two-pronged approach is necessary to elucidate these long-range interactions since they are, in part, elastically mediated by the substrate and because the detailed interactions between an adatom and the substrate are not described by the elastic theory.

It is possible to distinguish between two regimes of the interaction between surface steps and adatoms. The first one, which is observed when the distance between an adatom and a step is of the order of a few atomic diameters, has been studied both theoretically[4] and experimentally.[5] It has long been known that the presence of a step creates a diffusion barrier (so-called Shwoebel barrier) that prevents adatoms from migrating from an upper terrace to a lower terrace, across a step.[6] This phenomenon, as well as adatom diffusion along the step, has been studied using atomistic static relaxation[7] and molecular-dynamics[8] simulation methods, as well as by analyzing experimentally observed distribution of adatoms near the edge of an individual step.[9]

The second regime can be described as an interaction between defects that are far (many atomic diameters) apart from each other. These interactions are mediated by the underlying substrate. There are two distinct origins of this long-range interaction.[1] Perturbations of electronic structure in the vicinity of defects give rise to charge redistribution and therefore electrostatic forces between the defects.[10] Both adatoms and surface steps distort the underlying substrate, thereby setting up long-range elastic fields. The interaction between the elastic fields of these defects cause long-range defect-defect interactions. Although it is generally not possible to separate these two mechanisms from each other, understanding each of these individually will help clarify the nature of defect-defect interactions on surfaces. In the present paper, we focus on the elastic interactions.

Although the detailed elastic fields associated with surface defects may be very complex and are spread over a finite area of the surface (e.g., an adatom), at distances much greater than the spatial extent of the defect the elastic distortions of the underlying solid can be thought of as if created by a point source of tractions on the flat surface (linear tractions in the case of a linear defect). Therefore, it is possible to replace the actual defect by point or line tractions on the free surface and study the interactions between these defects by means of continuum elastic theory. In the present paper, we explicitly consider the case of a semi-infinite solid, which we model as an elastic half space occupying the region $z>0$, such that steps or adatoms on a surface are at $z=0$. Without loss of generality, we will assume that steps run in the y direction and an individual adatom is at the origin of the coordinate system.

A model of surface steps in terms of surface tractions was proposed by Marchenko and Parshin.[11] They suggested that the elastic field of a step is the same as that of an array of force dipoles uniformly distributed on the surface along the step line or, alternatively, a linear force dipole. The tractions $\mathbf{T}$, therefore, are independent of the coordinate y on the surface

$$\mathbf{T}_{\text{step}}(\rho)=\mathbf{D}\delta'(y), \tag{1}$$

where ρ is the shortest vector that connects a point on the surface to the step and $\delta'(y)$ is the derivative of the delta

function with respect to its argument. The direction and magnitude of the dipole vector **D** depend on the surface orientation and the material under investigation. The validity of Marchenko and Parshin's hypothesis was verified in a number of papers via the analysis of the interaction energy of similar parallel steps[12,13] and the actual step displacement field.[14]

Surface tractions simulating an adatom were considered in Refs. 15–17 as a sum of forces the adatom exerts on its neighboring atoms in the underlying solid. Since each component of the force must, on average, be zero and because they are central forces, they can be replaced by a force dipole. These tractions can, in general, be described by a symmetric dipole force tensor $\mathbf{A}_{\mu\nu}$,

$$\mathbf{T}_{\text{adatom}}(\rho)=\mathbf{A}_{\mu\nu}\frac{\partial}{\partial x_\nu}\delta(\rho),\quad \mu,\nu=x,y, \tag{2}$$

which is isotropic on a high-symmetry surface: $\mathbf{A}_{\mu\nu}=A\,\delta_{\mu\nu}$.[11,18] The component of the traction perpendicular to the surface was neglected since it results in terms that are higher order than dipole.

Modeling the elastic deformation of the material in terms of a dipole surface traction is an approximation since higher-order terms in the expansion of the elastic field in terms of multipoles may be important. This line or point dipole approximation for the field of surface defects also neglects the finite extent of the true surface defect ''core'' (i.e., the region in which the deformation cannot be described solely by linear elasticity). This nonlocality of the source of tractions may also result in the appearance of higher-order ''multipoles,'' which may be important. Nonelastic interactions may also be important at small defect separation (e.g., direct bonding interactions). Nonetheless, this line dipole approximation has proven to be adequate for modeling the elastic interactions between parallel surface steps for step separations larger than three atomic spacings in Ni.[14]

In the present paper, we examine the elastic interaction of a Ni adatom with a ⟨001⟩ step on a {100} Ni surface, described using an empirical interatomic potential. Our objective is to determine the appropriateness of the dipole elastic model for describing the adatom-step interaction at large separation and to parametrize the elastic model using results from the atomistic simulation. We begin by performing atomistic simulations of a square lattice of adatoms. The results of these simulations are analyzed in terms of continuum elasticity so that we may extract the magnitude of the force dipole A of an adatom. A serves as an input into the continuum elastic description of the interaction between an adatom and a ⟨001⟩ step. The magnitude of the linear force dipole **D** associated with a step was obtained in an earlier study.[14] We then perform a series of atomistic simulations in which we vary the adatom-step separation in order to determine the adatom-step interaction energy. Combining the results of these studies, we make a critical comparison of the atomistic and continuum elastic results.

II. ELASTIC ANALYSIS

The energy associated with the interaction of any two surface defects can readily be obtained once their corresponding surface traction distribution is determined. The elastic field associated with any distribution of surface tractions may be found by convoluting the tractions with the elastic surface Green's tensor **G** appropriate to the underlying medium:

$$\mathbf{u}(\rho,z)=\int d\rho'\,\mathbf{T}(\rho')\mathbf{G}(\rho-\rho',z), \tag{3}$$

where z is the coordinate normal to the surface. The energy of interaction between two defects E_{int} may be determined by a simple virtual work argument: i.e., it equals the force (traction) due to one defect times the displacement field of the other

$$E_{\text{int}}=\tfrac{1}{2}(\mathbf{T}_1\mathbf{u}_2+\mathbf{T}_2\mathbf{u}_1), \tag{4}$$

where $\mathbf{T}_i\mathbf{u}_j$ is the product of the surface displacement due to defect j evaluated at the position of defect i and the traction due to defect i. Using Eq. (3) and the reciprocal theorem $\mathbf{u}_T\,\mathbf{T}_2=\mathbf{u}_2\mathbf{T}_1$, Eq. (4) may be rewritten as

$$E_{\text{int}}=\int\int d\rho\;d\rho'\,\mathbf{T}(\rho)\mathbf{T}(\rho')\mathbf{G}(\rho-\rho',z=0), \tag{5}$$

where the double integral is evaluated over the entire surface.

For an isotropic medium, the surface elastic Green's function **G** is known in closed form.[19] If we model the traction distribution of an adatom as two perpendicular, in-plane surface force dipoles, the elastic interaction between adatoms as a function of their separation d_0 may be obtained directly from Eq. (5):[11]

$$E_{\text{int}}^{\text{ad}}=\frac{(1-\nu^2)}{\pi E}\frac{A^2}{d_0^3}, \tag{6}$$

where E and ν are Young's modulus and Poisson's ratio of the medium and A is the strength of the force dipole. The interaction between like adatoms is isotropic, repulsive, and decays as the cube of the reciprocal separation.

The energy associated with the interactions between an adatom and a surface step can be obtained from Eq. (4). In this case, it is convenient to rewrite Eq. (4) using the reciprocal theorem as

$$E_{\text{int}}=\mathbf{T}_{\text{adatom}}\mathbf{u}_{\text{step}}. \tag{7}$$

The elastic field of a step on the surface of an isotropic medium is well known and is described in detail in Ref. 20. The displacements decay away from the step as 1/r. In the isotropic case, the in-plane and out-of-plane components of the displacement vector are decoupled at the surface, i.e., the out-of-plane component of the force dipole **D** creates no in-plane component of the vector $\mathbf{u}_{\text{step}}$ and vice versa. Since the out-of-plane component of the surface tractions associated with the adatom are higher order than dipole, we neglect them. Therefore, we only need to consider the in-plane component of the displacement field of the step in Eq. (7). The dependence of E_{int} on the distance between a step and an adatom d_0 is obtained by replacing the dipole tractions associated with the adatom with its representation as a derivative of a δ function [see Eq. (2)]:

$$E_{\text{int}}^{\text{ad st}}=\frac{2(1-\nu^2)}{\pi E}\frac{\mathbf{D}_x A}{d_0^2}. \tag{8}$$

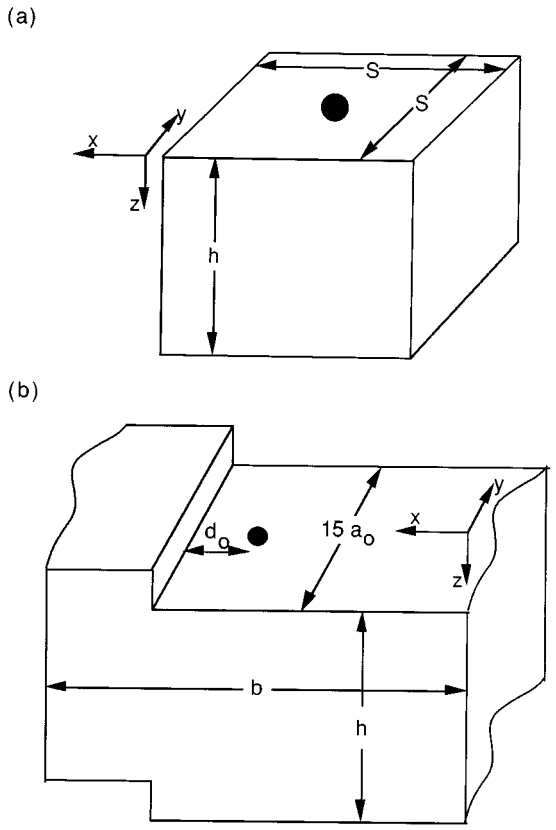

FIG. 1. Geometry of the simulation cells used to determine the (a) adatom-adatom interaction strength and the (b) step-adatom interaction strength. In both cases, periodic boundary conditions are imposed in the x and y directions.

Whether this interaction is repulsive or attractive is determined by the signs of both A and $\mathbf{D}_x$. Both these quantities can only be determined microscopically, i.e., in terms of the local atomic interactions in the core of each defect. The interaction energy within the linear elastic and dipole approximations is symmetric with respect to whether the adatom is on the upper or the lower terrace (to the left or right of the step) in Fig. 1(b). This is because the in- and out-of-plane components of the step force dipole and its displacement field are decoupled in this approximation.

The interaction energy between surface defects, which are each described in terms of a multipole (derivatives of a δ function), is inversely proportional to some power of their separation d_0.[21] Increasing the number of terms one uses in the multipole expansion of the defect surface traction adds additional terms in the defect interaction energy that are of higher order (i.e., higher powers of the inverse defect separation $1/d_0$) to the lowest-order description of the defect-defect interaction energy [e.g., Eqs. (6) and (8)]. In the cases of step-adatom and adatom-adatom interactions considered here, the leading-order term in the expansion of the surface tractions is of second order (i.e., dipole). Therefore, the leading-order term (i.e., smallest power of $1/d_0$) in the surface defect-defect interactions will always be a associated with dipole-dipole interactions. This effectively prohibits the appearance of a term linear in $1/d_0$ in Eq. (8) and terms linear or quadratic in $1/d_0$ in Eq. (6). This same conclusion holds in the anisotropic elasticity case as well, since the self-similarity of the displacement field created by a surface multipole is a consequence of the homogeneity of the underlying elastic equation of equilibrium.[16]

III. SIMULATION METHOD

In the present study, two independent series of atomistic simulations were conducted. In order to determine the magnitude of the elastic force dipole A of an adatom on the {001} Ni surface, we performed a series of simulations of a regular (square) lattice of adatoms on the otherwise flat {001} surface of Ni at several nearest-neighbor adatom separations S. The geometry of the computational cell used in these simulations is shown in Fig. 1(a). The periodically repeated simulation cell consists of a square unit cell on the (001) surface, with one adatom placed at its center. The adatom nearest-neighbor separation S was varied in the range $5a_0-22a_0$, where a_0 is the equilibrium face-centered-cubic Ni lattice constant. h denotes the depth of the computational cell in the z direction. At distances below $z=h$, all atoms were fixed in their perfect crystal lattice positions.

Next, we performed a series of atomistic simulations of a periodic array of adatoms on a vicinal surface consisting of [001] monoatomic height steps and (001) terraces. Several simulations were performed as a function of step–nearest-adatom spacings d_0 for the geometry shown in Fig. 1(b). In particular, we examined $4a_0 \leqslant d_0 \leqslant 9.5a_0$ for adatom separations of $15a_0$ in the direction parallel to the steps and b in the direction perpendicular to the steps. The interstep separation was also fixed at $b=50a_0$. In all cases, the separation between adatoms and between adatoms and non-nearest steps are assumed to be sufficiently large such that their mutual interactions are predominantly elastic in nature. In practice, all of the periodicities are imposed by the application of periodic boundary conditions in the $0X$ and $0Y$ directions.

The interatomic interactions were modeled by the embedded-atom method (EAM) potentials proposed by Daw and Baskes in Ref. 22. In this approach, the total energy of the system may be written in terms of two distinct terms: the first is a pairwise interaction φ (which is mainly repulsive) and the second is an on-site ''embedding'' energy F, which is a function of pairwise contributions ρ from other atomic sites:

$$E_{\text{total}}=\tfrac{1}{2}\sum_{i,j}^{N}\varphi(r_{ij})+\sum_{i}^{N}F\left(\sum_{j\neq i}\rho(r_{ij})\right). \tag{9}$$

Here r_{ij} is the distance between atoms i and j and N is the total number of particles in the system. F, φ, and ρ are empirical functions chosen to fit certain thermodynamic parameter of a perfect Ni crystal (lattice constant, vacancy formation energy, universal binding energy curve, and elastic bulk modulus). Analytical expressions for these functions can be found in Ref. 23.

The equilibrium configuration of the system was determined by minimizing the total energy [Eq. (9)] with respect to the positions of all of the atoms. This minimization was performed using the conjugate gradient method.[24] This minimization procedure was stopped when the residual force on all atoms was less than or equal to 10^{-5} eV/a_0. This corresponds to a relative error in the determination of the total

energy of 10^{-7} for a lattice of adatoms and 10^{-5} in the step-adatom simulations. In order to ensure that the perfect crystal to which the finite-size simulation cell was matched at $z=h$ had no influence on the adatom-adatom interaction energies, h was increased until the interaction energies did not change to the desired precision. In the step-adatom interaction simulations, h was fixed at $12.5a_0$. This depth is greater than the largest step-adatom spacing examined.

IV. RESULTS AND DISCUSSION

A. Interactions between adatoms

In the present study, we perform atomistic simulations of adatom-adatom interactions in order to determine the magnitude of the adatom force dipole A, which sets the magnitude of the adatom-adatom interactions energy within the elastic theory [Eq. (6)]. The present simulations were performed using a square lattice of adatoms on the (001) surface of Ni. In order to analyze these simulation results, we must first extend Eq. (6) in order to determine an expression for the interaction energy associated with a square lattice of adatoms. The interaction energy per adatom in the square lattice of adatoms is

$$E_{\rm int}^{\rm ad}=\tfrac{1}{2}\sum_i E_i=\tfrac{1}{2}\sum_i \frac{(1-\nu^2)}{\pi E}\frac{A^2}{d_i^3}, \tag{10}$$

where E_i is the energy of the interaction of an adatom at the origin with the ith adatom [Eq. (6)] and d_i is the adatom separation. The factor of one-half in Eq. (10) may be traced to Eq. (4) and the reciprocal theorem. Rewriting Eq. (10) in terms of the indices (m,n) associated with each adatom in the square lattice yields

$$E_{\rm int}^{\rm ad}=\frac{1}{2}\frac{(1-\nu^2)}{\pi E}\frac{A^2}{S^3}\sum_{m,n}\frac{1}{(m^2+n^2)^{3/2}}=\frac{K}{2}\frac{(1-\nu^2)}{\pi E}\frac{A^2}{S^3}, \tag{11}$$

where S is the period of the nearest-neighbor adatom spacing in the lattice and the summation is over all adatoms (excluding the origin). We denote the summation in Eq. (11) as K and find that $K\approx 9.03$. Equation (11) provides an analytical basis that we can use to extract the magnitude of the adatom force dipole A from the simulation results.

In the atomistic simulations of adatom-adatom interactions, we determine the total energy for one unit cell of the square lattice of adatoms as a function of the adatom spacing S. The total energy per cell consists of four terms

$$E_{\rm tot}=E_{\rm bulk}+E_{\rm surf}+E_{\rm ad}+E_{\rm int}^{\rm ad}. \tag{12}$$

The first term $E_{\rm bulk}$ corresponds to the bulk energy, which is the product of the energy of an atom in a perfect crystal and the number of atoms in the computational cell. The surface energy $E_{\rm surf}$ is the energy per unit area of the surface times S^2. The third term $E_{\rm ad}$ is the difference in energy between an infinite surface with and without a single adatom. Finally, the adatom interaction energy $E_{\rm int}^{\rm ad}$ corresponds to the interaction between one adatom and all other adatoms in the adatom lattice, as per Eq. (11). $E_{\rm bulk}$ is simply the sublimation energy of Ni, which is an input parameter used to determine the EAM potential used in these studies. The surface energy was determined using the same interatomic potential, as described in Ref. 25. $E_{\rm ad}$ was determined by extrapolating a plot of $E_{\rm tot}-E_{\rm bulk}-E_{\rm surf}$ versus the cube of the inverse adatom spacing to $1/S^3=0$, since $E_{\rm int}^{\rm ad}$ must go to zero as $1/S^3$. Using these parameters, we plot $E_{\rm int}^{\rm ad}=E_{\rm tot}-E_{\rm bulk}-E_{\rm surf}-E_{\rm ad}$ versus S^{-1} and S^{-3} in Figs. 2(a) and 2(b), respectively, for $8a_0\leqslant S\leqslant 23a_0$.

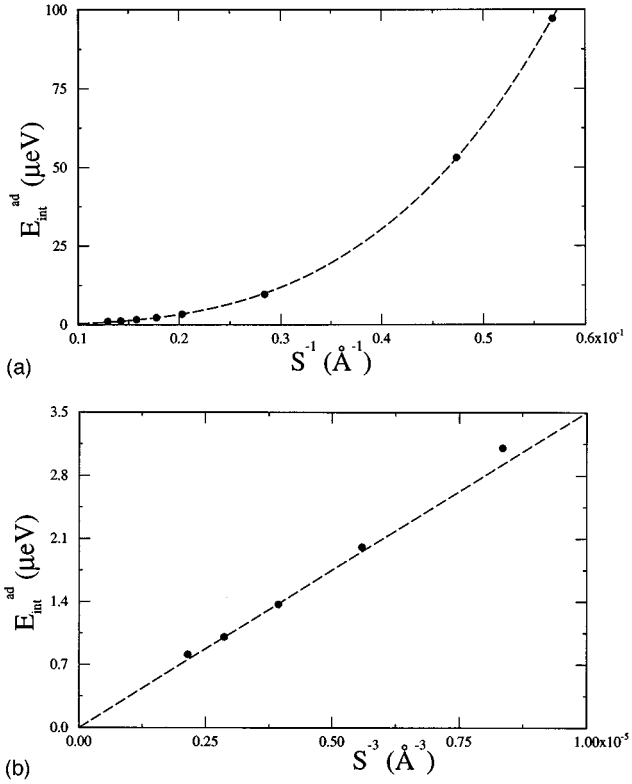

FIG. 2. Adatom-adatom interaction energies for adatoms on the (001) surface of EAM Ni versus (a) the inverse nearest-neighbor adatom separations S^{-1} and (b) the inverse cube of the nearest-neighbor adatom separations S^{-3}. The dashed line in (a) corresponds to Eq. (13) with $n_{\rm max}=4$ the data in Table I. The dashed line in (b) corresponds to Eq. (13), where we have used only the A_3 term in the $n_{\rm max}=4$ fit in Table I.

In order to evaluate the accuracy of the elastic force dipole model for adatom interaction, we fit the data presented in Fig. 2(a) to the functional form

$$E_{\rm int}^{\rm ad}=\sum_{n=3}^{n_{\rm max}}\frac{A_n}{S^n}, \tag{13}$$

where the A_n are fitting constants. This functional form was chosen because it represents a multipole expansion of the adatom interaction energy. This sum starts at $n=3$ because $n=3$ corresponds to the lowest-order adatom interaction, i.e., dipole-dipole interactions as discussed above. The higher-order terms in Eq. (13) represent dipole-quadropole, quadropole-quadropole, etc., terms in the expansion. Table I shows the results of this fit for the cases $n_{\rm max}=3$ and 4. The data were not sufficiently precise to allow the meaningful extraction of higher-order multipoles. Table I shows that the third-order (dipole-dipole) term is dominant for $S>A_4/A_3=10.3$ Å; nonetheless, the fourth-order (dipole-quadropole) term is very significant for the range of S exam-

TABLE I. Parameters describing adatom-adatom interactions on a (100) surface of EAM Ni, obtained by fitting the data in Fig. 2(a) to the functional form in Eq. (13). The series expansion describing these interactions was terminated after one term ($n_{max}=3$) and after two terms ($n_{max}=4$).

n_{max}	A_3 (eV Å^3)	A_4 (eV Å^4)
$n_{max}=3$	0.53	
$n_{max}=4$	0.34	3.4

ined here ($8a_0 \leqslant S \leqslant 22a_0$, $a_0=3.52$ Å). The dominance of the dipole-dipole term may also be seen by fitting the adatom interaction energy data to the general form

$$E_{int}^{ad}=\frac{A_\alpha}{S^\alpha}. \tag{14}$$

The resulting fit yields $\alpha=3.34\pm0.01$, which again shows that while the leading-order interaction is dipole-dipole, the higher-order terms are significant and cannot be omitted.

Although the present results represent a strong argument in favor of the dipole model [Eq. (11)], a non-negligible deviation exists. This deviation may be traced to several factors. First, the present surface force description of the elastic field of an adatom ignores the fact that the adatom can interact directly with some of the atoms below the surface. In the present EAM simulations, atomic interactions extends to third-nearest-neighbor shells. Incorporating these finite-extent interactions into the continuum theory would lead into higher-order terms in the multipole expansion.

Another possible explanation of the deviation of the adatom interaction results from the predictions of the dipole model is associated with neglecting out-of-plane components of the surface force. Such out-of-plane forces must, by symmetry, be represented only by even functions. Hence the lowest-order term in the out-of-plane surface force must correspond to the second derivative, a δ function, which corresponds to a quadropole surface force. This justifies the appearance of a fourth- (and higher-) order term in the multipole expansion described by Eq. (14).

We can use the results of the dipole model and the atomistic simulations to determine the magnitude of the atomic force dipole A. Comparing Eqs. (11) and (13) in the dipole limit [i.e., $n_{max}=3$ in Eq. (13)], we obtain the following relationship between A_3 and the atomic force dipole A:

$$A=\left(\frac{2\pi E}{(1-\nu^2)K}A_3\right)^{1/2}. \tag{15}$$

Using the data in Table I for $n_{max}=4$, we obtain an estimate for the numerical value of A: $A=0.62$ eV. In this calculation, we used the isotropic elastic constants E and ν appropriate for the EAM potential for Ni used in the present simulations. These elastic constants represent the Voigt average of three anisotropic cubic elastic constants.

Equation (15) gives only the absolute value of the force dipole A. Its sign (i.e., whether the dipole exerts a compressive or a tensile stress on the surface) was determined by analyzing surface atomic displacements in the vicinity of the adatom. Displacements of atoms closest to the center of the defect are directed outward (corresponding to compression at the surface), leading us to assign a negative value to the force dipole strength.

The value of the adatom, surface force dipole strength can now be used to evaluate the continuum elastic results for the interaction energy of adatoms and other types of surface defects with a known surface displacement field. In the next subsection, we analyze the elastic interactions between Ni adatoms and ⟨100⟩ steps on the {001} nickel surface.

B. Step-adatom interactions

The elastic interaction energy between a nickel adatom and a ⟨100⟩ step on the {001} surface can be estimated with the aid of Eq. (8). However, before proceeding with this analysis, we first investigate the effects of the significant elastic anisotropy of Ni.

An anisotropic elastic analysis of the displacement field of a ⟨100⟩ step on the {001} surface was carried out in Ref. 14. The in-plane component of the displacement field of a step in the dipole approximation was shown to be

$$\mathbf{u}_x^{step}=-\mathbf{D}_x/\pi L d_0, \tag{16}$$

where $\mathbf{D}_x$ is the magnitude of the in-plane component of the step force dipole, d_0 is the distance from the step, and L is the anisotropic version of the factor $E/[2(1-\nu^2)]$ that appears in the isotropic expression, Eq. (8). The expression for L involves a combination of all three elastic constant of a cubic crystal C_{11}, C_{12}, and C_{44}, and its numerical value for the ⟨100⟩ step on the {001} surface of EAM nickel is 0.627 eV/Å^3.[14] For a step of this orientation, the anisotropic elastic correction to the adatom/step interaction [Eq. (8)] becomes

$$E_{int}^{ad\text{-}st}=\frac{1}{\pi L}\frac{\mathbf{D}_x A}{d_0^2}, \tag{17a}$$

where

$$L=\frac{C_{44}(C_{11}-C_{12})}{\sqrt{\left(4\frac{C_{11}C_{44}}{C_{11}+C_{12}}+H\right)\left(\frac{C_{11}C_{44}}{C_{11}+C_{12}}\right)}} \tag{17b}$$

and H is the elastic anisotropy of the cubic crystal: $H=C_{11}-C_{12}-2C_{44}$.

In an earlier atomistic simulation study,[14] we found that the magnitude of the in-plane component of the step force dipole $\mathbf{D}_x$ is equal to -0.15 eV/Å. (There is a difference in sign with Ref. 14 associated with the handedness of the coordinate system.) Combining this result, the magnitude of the surface dipole strength associated with the adatom, and Eq. (17) yields the adatom-step interaction energy with no adjustable parameters. Therefore, we can use this result to directly analyze the adatom/step interactions found in the atomistic computer simulations. Using the independently determined defect strengths ($A<0$ and $\mathbf{D}_x<0$), the step/adatom interactions [Eq. (17)] are repulsive and are symmetric with respect to the position of an adatom about the step. This same conclusion was found in the isotropic limit [Eq. (8)] as well. Corrections to Eq. (17) may result from terms higher than dipole in the expansion of the surface tractions

simulating either and/or both of the defects. These corrections will be terms including cubic and higher powers of the reciprocal distance d_0 between a step and an adatom.

The presence of the periodic boundary conditions in the atomistic simulations prevents us from directly applying Eq. (17) to the simulation data. Fortunately, we can rederive Eq. (17) for the case of an adatom interacting with a periodic array of steps results:

$$E_{\text{int}}^{\text{ad-st}} = \frac{\pi^2}{b^2 \sin^2\left(\frac{\pi d_0}{b}\right)} \frac{\mathbf{D}_x A}{\pi L}, \tag{18}$$

where b is the interstep spacing in the computational cell. The next-higher-order term in the expansion of the step/adatom interaction will transform into a term proportional to

$$\frac{\pi^3 \cos\left(\frac{\pi d_0}{b}\right)}{b^3 \sin^3\left(\frac{\pi d_0}{b}\right)}.$$

The results of the simulations for both the upper and the lower terraces of the step were fitted to the functional form

$$E_{\text{int}}^{\text{ad-st}} = B_1 \frac{\pi^2}{b^2 \sin^2\left(\frac{\pi d_0}{b}\right)} + B_2 \frac{\pi^3 \cos\left(\frac{\pi d_0}{b}\right)}{b^3 \sin^3\left(\frac{\pi d_0}{b}\right)}, \tag{19}$$

where B_1 and B_2 are fitting constants. There is an uncertainty, of order of the size of the core of the step, as to which point corresponds to the appropriate origin of the coordinate system. For the sake of simplicity, we measured d_0 from the adatom position to the step along the terrace. In other words, for adatoms on the upper terrace, d is measured to the top of the step, and on the lower terrace, d is measured to the bottom of the step.

The dependence of the step-adatom interaction energy on step-adatom separation d_0 for adatoms on both the upper and lower terraces, obtained from the atomistic simulations, is shown in Fig. 3. Over the range of step-adatom separations considered here ($4a_0 \leqslant d_0 \leqslant 9.5a_0$) with an interstep separation fixed at $b = 50a_0$, the step-adatom interaction energy decays monotonically. This figure also shows that there is a difference between the step-adatom interaction energies for adatoms on the upper and lower terraces. This difference is largest at small separations and becomes negligible (within the numerical error) at large separations. At small separations, the adatom-step repulsion is larger on the upper terrace.

Table II shows the results of the determination of the parameters B_1 and B_2 in Eq. (17) by fitting to the simulation data in Fig. 3. The values of the dipole-dipole coefficient B_1, determined from the simulation data for the upper and lower terraces, are in good agreement (i.e., $B_1 = 112 \pm 13\%$). On the other hand, the values corresponding to the dipole-quadropole coefficient. B_2 differ by approximately 300% and are both attractive (negative). This deviation can also be seen in Fig. 3, where the two curves representing the upper and lower terraces deviate from each other in regions of small step-adatom separation. The large differences in the third-order term in the expansion of the step-adatom interaction [Eq. (19)] are due, in part, to the antisymmetry of the out-of-plane (vertical) component of the displacement field of the step. This antisymmetry only enters the dipole-quadropole and higher-order terms since the leading-order term in the out-of-plane surface force of the adatom is quadropolar, while that of the step is dipolar. Normally, we would expect that these terms would lead to opposite signs of B_2 on the upper and lower terraces. However, there are also other dipole-quadropole terms present associated with higher moments of the in-plane force distribution and the non-point-like spatial distribution of those force distributions. In the range of separations presented in Fig. 3, the contribution to the interaction energy of these third-order terms is approximately 5% for the upper terrace and 20% for the lower terrace.

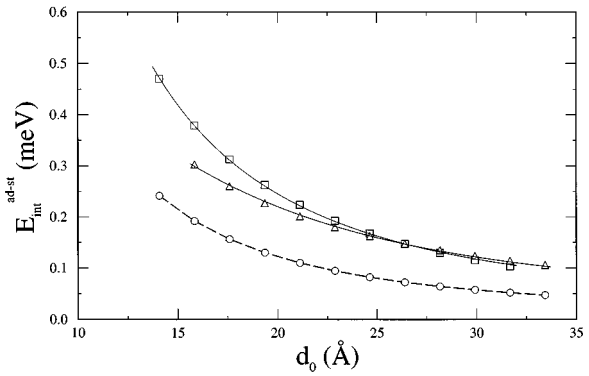

FIG. 3. Step-adatom interaction energy for the case of a (001) surface with [100] steps in EAM Ni. The data indicated by the squares and triangles correspond to adatoms on the terraces immediately above and below the step, respectively. The dashed line is calculated according to Eq. (18) with no adjustable parameters. The solid lines correspond to the best fit of the data to Eq. (19).

Figure 3 also shows a comparison of the step-adatom interaction energies determined from the simulations with those predicted by the elastic theory (where we have independently determined all of the parameters). The predicted step-adatom interaction energy and those from the simulations show very nearly the same separation (d_0) dependence. This suggests that the dipole surface force model for step-adatom interactions is valid. However, the simulation results are shifted to higher step-adatom interaction energies as

TABLE II. Parameters describing the interactions between a [100] step on a (100) surface and an adatom. These parameters were obtained by fitting the data in Fig. 3 to the functional form in Eq. (19). The data point labeled ''elastic theory'' was obtained from Eq. (18) using the dipole strengths determined from simulations based on isolated defects.

	B_1 (meV Å^2)	B_2 (meV Å^3)	χ^2
elastic theory	46.9		
upper	99.3	−109.9	3.65×10^{-5}
lower	124.5	−837.4	5.89×10^{-5}

compared to the theoretical predictions by approximately a factor of 2.5. We believe that the error here is primarily associated with the neglect of the elastic anisotropy in treating the elastic field of the adatom. Inclusion of this anisotropy is expected to significantly increase the value of the adatom dipole strength A.

In the dipole approximation to the elastic field of an adatom, the isotropic elastic theory predicts that an adatom produces an elastic displacement field that is independent of the angle in the plane of the surface and decays away from a dipole as the square of the reciprocal distance d_0. In this approach, the adatom-adatom interaction energy is isotropic and the adatoms repel each other. The presence of elastic anisotropy significantly modifies these results. While the d_0^{-3} self-similarity of the interaction energy [Eq. (6)] is preserved, the magnitude of the energy itself and even its sign may show a pronounced dependence on the orientation of the vector connecting an adatom to another adatom with respect to the crystallographic axis of the material.[26]

Dobrzynski and Maradudin[16] obtained an expression for the Fourier transform of the anisotropic elastic surface Green's function and derived the Green's function itself for the case of the free surface parallel to the basal plane in hexagonal crystal. No similar closed-form expression was found for the case of a crystal with cubic symmetry.[17] Using the approach followed in Ref. 16 and numerical evaluation of the necessary integrals, Lau[27] computed the angular dependence of the interaction energy of a pair of Xe adatoms on the (001) faces of a number of fcc metals, including nickel. His results show that the interaction energy has a fourfold symmetry: It is large and repulsive for ⟨110⟩ oriented adatom pairs and weak and attractive for ⟨100⟩ oriented adatom pairs. Kappus used an eigenfunction approach[28] to determine the interaction energy associated with a pair of adatoms in the form of a rapidly converging sum. He also found that the interaction energy of adatoms on a (001) surface of an anisotropic material may be attractive along certain crystallographic directions. Inclusion of these anisotropy effects would substantially increase the magnitude of the adatom dipole strength, which we determined by making a comparison with adatom-adatom interaction simulations.

V. CONCLUSION

We derived an analytical expression for the interaction energy in the framework of linear elasticity. There are two unknowns in this theory: the strength of the elastic fields associated with the adatoms and with the steps. In order to determine these parameters independently, we performed a series of atomistic simulations of a square lattice of Ni adatoms on the (001) Ni surface using EAM potentials. The results were analyzed in terms of a dipole model for an adatom and were shown to be in good agreement with the elastic theory. By fitting these simulations to the theory we were able to extract the magnitude of the force dipole of an adatom. In a separate study, we used the same general approach to determine the magnitude of the surface force dipole associated with a surface step. These defect strengths were used to predict the elastic interaction energy between a Ni adatom and a ⟨001⟩ step on the same surface. Atomistic simulations of a surface with a periodic array of steps interacting with an adatom were performed and compared with the predictions of the elastic theory with no adjustable parameters. A detailed comparison of the simulation and theoretical result showed that the step-adatom interactions were dominated by dipole-dipole interactions, but that higher-order terms can also be significant in the range of adatom-step separation studied here. However, the absolute magnitude of the step-adatom interaction energy showed that there were significant errors. We believe that these errors are associated with the neglect of anisotropic effects in the elastic analysis used to extract that adatom dipole strength.

ACKNOWLEDGMENTS

We would like to express our gratitude to Professor R. Eykholt for his help in analytical evaluation of constant K in Eq. (11). Further, we gratefully acknowledge the Division of Materials Science of the Office of Basic Energy Sciences of the United States Department of Energy, Grant No. FG02-88ER45367, for its support of this work.

[1] T. L. Einstein, in *Handbook of Surface Science: Physical Structure, Vol. 1*, edited by W. N. Unertl (North-Holland, Amsterdam, 1996).
[2] C. Duport, P. Politi, and J. Villain, J. Phys. (France) I **5**, 1317 (1995).
[3] G. Ehrlich, Surf. Sci. **246**, 1 (1991).
[4] Chun-Li Liu, Intern. J. Mod. Phys. B **9**, 1 (1995).
[5] G. Ehrlich, Surf. Sci. **331**, 865 (1995).
[6] R. L. Schwoebel and E. J. Shipsey, J. Appl. Phys. **37**, 3682 (1966).
[7] Chun-Li Liu and J. B. Adams, Surf. Sci. **294**, 197 (1993).
[8] C. Uebing, Phys. Rev. B **49**, 13 913 (1994).
[9] S. C. Wang and G. Ehrlich, Phys. Rev. Lett. **71**, 4174 (1993).
[10] W. Kohn and K. H. Lau, Solid State Commun. **18**, 553 (1976).
[11] V. I. Marchenko and A. Ya. Parshin, Zh. Eksp. Teor. Fiz. **79**, 257 (1980) [Sov. Phys. JETP **52**, 129 (1980)].
[12] D. Wolf and J. A. Jasczak, Surf. Sci. **277**, 301 (1992).
[13] R. Najafabadi and D. J. Srolovitz, Surf. Sci. **317**, 221 (1994).
[14] L. E. Shilkrot and D. J. Srolovitz, Phys. Rev. B **53**, 11 120 (1996).
[15] K. H. Lau and W. Kohn, Surf. Sci. **65**, 607 (1977).
[16] L. Dobrzynski and A. A. Maradudin, Phys. Rev. B **14**, 2200 (1976).
[17] K. Portz and A. Maradudin, Phys. Rev. B **16**, 3535 (1977).
[18] W. Kappus, Z. Phys. B **29**, 239 (1978).
[19] L. D. Landau and E. M. Lifshitz, *Theory of Elasticity*, 3rd ed. (Pergamon, Oxford, 1986).
[20] J. Stewart, O. Pohland, and J. M. Gibson, Phys. Rev. B **49**, 13 848 (1994).
[21] J. M. Rickman and D. J. Srolovitz, Surf. Sci. **284**, 211 (1993).

[22] M. S. Daw and M. I. Baskes, Phys. Rev. B **29**, 6443 (1984).
[23] S. M. Foiles, M. L. Baskes, and M. S. Daw, Phys. Rev. B **33**, 7983 (1986).
[24] W. H. Press *et al.*, *Numerical Recipes in C: The Art Of Scientific Computing*, 2nd ed. (Cambridge University Press, New York, 1992), pp. 420–425.
[25] S. P. Chen, A. F. Voter, and D. J. Srolovitz, J. Mater. Res. **4**, 62 (1989).
[26] A. M. Stoneham, Solid State Commun. **24**, 425 (1977).
[27] K. H. Lau, Solid State Commun. **28**, 757 (1978).
[28] W. Kappus, Z. Phys. B **45**, 113 (1981), and references therein.